A QUARK MODEL FOR HADRON PRODUCTION*

H. MÜLLER **

Institut für Kern- und Hadronenphysik, Forschungszentrum Rossendorf,
Postfach 510119, D-01314 Dresden, Germany
E-mail address: muellerh@fz-rossendorf.de

(Received October 9, 1996)

Hadron production in nucleon-nucleon, nucleon-nucleus and nucleus-nucleus interactions is considered in the framework of the Rossendorf collision model, which aims at describing simultaneously all reaction channels in a wide energy region. An empirical matrix element based on the partonic picture of hadrons is combined with the concept of intermediate subsystems and the calculation of modified statistical weights of the various final states. In case of nuclear reactions the Glauber concept is used to calculate the partial cross sections for the interaction of various numbers of participants. It is demonstrated that a large variety of experimental data can be satisfactorily reproduced. Predictions for proposed missing-mass measurements are discussed.

PACS numbers: 25.40. Ve, 25.10. +s, 25.90. +k

1. Introduction

The cooler synchrotron COSY with its excellent beam quality is a powerful tool to investigate all kinds of proton-induced reactions. Because of the complexity of the detection systems at COSY a careful optimization of the planned experiments by means of simulation calculations is necessary. In this context the prediction of the cross section to be measured as well as a good overall description of all the open reaction channels is needed. An improved version of the Rossendorf Collision (ROC) model [1, 2, and references therein] used earlier to consider various aspects of proton induced-reactions is adapted to this task. It is implemented as a Monte-Carlo code, which samples complete events. This offers the desired possibility to estimate the relation between the reaction of interest and the physical background.

* Presented at the "Meson 96" Workshop, Cracow, Poland, May 10–14, 1996.
** Supported by the Bundesministerium für Bildung, Wissenschaft, Forschung und Technologie under contract No. 06 DR 666 I.

2. The ROC model

In the ROC model nucleon-nucleon (NN), nucleon-nucleus (NA) and nucleus-nucleus (AA) interactions are considered in a unified approach, which aims at describing simultaneously all open reaction channels in a wide energy region. The interaction process is assumed to proceed via the creation of intermediate subsystems (called fireballs, clusters or clans in the literature). This concept is closely related to the partonic structure of the interacting particles. Subsystems are created in a first step of the interaction process and decay subsequently into the final reaction products. The discussion of such intermediate systems has a long history (see *e.g.*the reviews of Feinberg [3, 4]). Their existence is well established by the observation of short-range correlations [5] and finds a natural explanation in a spectator-participant picture of the interaction process at high energies where the participating partons form the central and the spectators the leading subsystems. In the context of the ROC model the term "cluster" is used for denoting these hadronic subsystems.

The final channels are selected by creating an arbitrary number of quark-antiquark ($q\bar{q}$) pairs. The final hadrons are then built up by randomly combining the available quarks. In this way all possible final channels allowed by conservation of internal quantum numbers are populated.

In case of nuclear interactions the partial cross sections for the interaction of various numbers of participants are calculated in the Glauber approximation of straight-line motion [6].

2.1. Nucleon-nucleon interactions

The relative probability of populating a channel α is calculated as the product of the Lorentz-invariant phase-space factor $\mathrm{d}L_n(s;\alpha)$ with the square of an empirical matrix element A^2, which describes the dynamics of the interaction process

$$\mathrm{d}W(s;\alpha) \propto \mathrm{d}L_n(s;\alpha)\, A^2 \,. \tag{1}$$

Here, $s = p^2$ denotes the square of the total energy with p being the total four-momentum, and a channel α is defined by the number n and masses m_i of the final particles. The Lorentz-invariant phase-space factor is defined as the integral over the momenta of the final particles with energy and momentum conservation taken into account

$$\mathrm{d}L_n\,(s;\alpha) = \mathrm{d}L_n\,(s;m_1,\ldots,m_n) = \prod_{i=1}^{n} \frac{\mathrm{d}^3 p_i}{2e_i}\, \delta^4(p - \sum_{i=1}^{n} p_i)\,. \tag{2}$$

The four-momentum of the i-th particle is denoted by $p_i = (e_i, \vec{p}_i)$ with $p_i^2 = m_i^2$. For numerical calculations the δ function in Eq. (2) must be

removed by introducing a new set of $3n - 4$ variables to replace the $3n$ momentum components. It is reasonable to choose a set of variables, which reflects the underlying physical picture of the interaction process. These variables appear also in the matrix element used to modify the phase-space factor.

The interaction process is assumed to proceed in several steps. In dependence on the incidence energy the first step results in the creation of a varying number of clusters. At low energies only two clusters with invariant masses M_1 and M_2 emerge from the interaction process. The interaction can be imagined to proceed via color-exchange between two quarks of the interacting particles (see for example [7]). With regard to the relatively low energies considered here the resulting "strings" are assumed to decay isotropically in their rest systems. The valence quarks of the interacting particles are distributed between the two excited clusters in dependence on the quark pair which has undergone the color-exchange. Additional $q\bar{q}$ pairs may be created in each cluster. With increasing energy the partonic substructure of the interacting hadrons becomes more and more important with the result that two leading spectator- and an arbitrary number of participant-clusters are produced. Each spectator contains in the case of a baryon-baryon interaction, as a rule, a valence di-quark, while the residual valence quarks and a random number of $q\bar{q}$ pairs are distributed in such a way that color neutral clusters are produced.

The variables introduced for decomposing the phase-space factor are the invariant masses

$$M_I = \sqrt{P_I^2} = \sqrt{\left(\sum_{i=1}^{n_I} p_i\right)^2} \quad I = 1, \ldots, N \tag{3}$$

of the N produced clusters and the four-momenta $t_{a1} = (p_a - P_1)^2$ and $t_{b2} = (p_b - P_2)^2$ transferred between the incident particles a and b and the leading clusters 1 and 2 as well as the transverse momenta $\vec{Q}_I$ of the participant-clusters $3 \ldots N$. Here, the four-momenta of clusters are denoted by capital letters P_I.

The subsequent decay of excited clusters in the second step of the interaction process leads to the production of primary particles by randomly combining the quarks available in each cluster. Resonances among the primary particles decay later into stable particles.

The dynamical input of the model is according to

$$A^2(\vec{\alpha}_N) = A^2_{\mathrm{ex}}(\vec{\alpha}_N) A^2_{\mathrm{sc}}(\vec{\alpha}_N) A^2_{\mathrm{qs}}(\vec{\alpha}_N) A^2_{\mathrm{st}}(\vec{\alpha}_N) \tag{4}$$

split into factors describing various aspects of the interaction process.

Cluster creation is treated on the basis of thermodynamical considerations. This is realized by using as matrix element the function

$$A^2_{\rm ex}(\vec{\alpha}_N) = \prod_{I=1}^{N} (M_I/\Theta_I) K_1(M_I/\Theta_I)\,, \tag{5}$$

which is the kernel of the so-called K-transformation (see [8]) used to transform a micro-canonical phase-space distribution depending on the total energy M_I of the I-th cluster into a canonical one, which is characterized by a temperature Θ_I. In Eq. (5) K_1 stands for the modified Hankel function. For increasing invariant masses M_I the function $(M_I/\Theta_I)K_1(M_I/\Theta_I)$ strongly decreases, while the phase-space factor $L_{n_I}(M_I)$ of the I-th cluster increases. This results in a maximum at a value of M_I determined by the parameter Θ_I. Thus, it is the temperature Θ_I which determines the average mass of the I-th cluster.

The cluster distribution in the phase-space is determined by the function

$$A^2_{\rm sc}(\vec{\alpha}_N) = \exp\left(\beta\,(t_{a1} + t_{b2})\right) \prod_{I=3}^{N} \exp\left(-\left(Q_I/\overline{Q_I}\right)^2\right), \tag{6}$$

which restricts the four-momentum transfer to the leading clusters via the slope parameter β (see *e.g.*Goulianous [9]) and the transverse momenta of the central clusters via a Gaussian containing the mean transverse momentum $\overline{Q}_I$ of the I-th cluster as parameter (see *e.g.*[10]).

The factor $A^2_{\rm qs}(\vec{\alpha}_N)$ in Eq. (4) represents the algorithm for selecting the decay channels on the basis of the quark picture of hadrons. In addition to the valence quarks of the initial particles up, down and strange quarks are produced in the ratio $u : d : s = 1 : 1 : \lambda$ with λ being the strangeness suppression factor due to the heavier mass of the strange quark. Thus, each cluster is viewed as a color-neutral system consisting of a certain number of quarks. The final hadrons are built up by randomly selecting sequences of quarks and anti-quarks. Each sequence is transformed into a hadron according to the rule that a $q\overline{q}$ gives a meson, while baryons or antibaryons are formed from qqq or $\overline{q}\overline{q}\overline{q}$. A discussion and theoretical foundation of the quark-statistics can be found by Anisovich and Shekhter [11]. The meson nonets with angular momenta zero and one $({}^1S_0, {}^3S_1, {}^1P_1, {}^3P_0, {}^3P_1, {}^3P_2)$ as well as all baryons with masses up to about 1.7 GeV [12] are used for building-up the primarily produced hadrons. In the present approach an empirical probability distribution

$$P(m) \propto \exp\left(-m/\Theta_I\right) \tag{7}$$

(see also [13]) is used to suppress the formation of heavier hadrons in accordance with the experimental findings. In Eq. (7), m is the mass of the final hadron and Θ_I is given in Eq. (5).

Finally, all factors still necessary for a correct counting of the final states are collected in the term

$$A^2_{\rm st}(\vec{\alpha}_N) = \left\{\prod_{I=1}^{N} g(\alpha_I)\left(\frac{V_I}{(2\pi)^3}\right)^{n_I-1} \left[\prod_{i=1}^{n_I}(2\sigma_i+1)2m_i\right]\right\}\left(\frac{V_N}{(2\pi)^3}\right)^{N-1} \tag{8}$$

It contains the spin degeneracy factors $(2\sigma_i+1)$, the volumes V_N in which the N clusters and V_I in which the particles arising from the I-th cluster are produced with $V_J = 4\pi R_J^3/3$ determined by the radius parameter R_J ($J = I$ or N). The quantity $g(\alpha_I) = \left(\prod_\beta n_\beta!\right)^{-1}$ prevents multiple counting of states for groups of n_β identical particles in the final state of the cluster I.

By defining the number of states in the decay channel α_I of one cluster

$$\mathrm{d}\mathcal{Z}_I(\alpha_I) = g(\alpha_I)\left(\frac{V_I}{(2\pi)^3}\right)^{n_I-1}\left\{\prod_{i=1}^{n_I}(2\sigma_i+1)2m_i\right\} \mathrm{d}M_I\left(\frac{M_I}{\Theta_I}\right)K_1\left(\frac{M_I}{\Theta_I}\right)\mathrm{d}L_{n_I}(M_I;\alpha_I) \tag{9}$$

and the analogous number of "cluster states"

$$\mathrm{d}\mathcal{Z}_N(s) = \left(\frac{V_N}{(2\pi)^3}\right)^{N-1}\left\{\prod_{I=1}^{N}(2M_I)\right\} \left\{\exp\left(\beta(t_{a1}+t_{b2})\right)\prod_{I=3}^{N}\exp\left(-(Q_I/\overline{Q_I})\right)\right\} \mathrm{d}L_N(s;M_1,\ldots,M_N) \tag{10}$$

the probability of populating the channel $\vec{\alpha}_N = (\alpha_1,\ldots,\alpha_N)$ [see Eq. (1)], follows as

$$\mathrm{d}W(s;\vec{\alpha}_N) \propto \left\{\prod_{I=1}^{N}\mathrm{d}\mathcal{Z}_I(\alpha_I)\right\}\mathrm{d}\mathcal{Z}_N(s)\,. \tag{11}$$

The physical quantities of interest can be derived from the differential cross section

$$\mathrm{d}\sigma(s;\vec{\alpha}_N) = \sigma_{\rm in}(s)\frac{\mathrm{d}W(s;\vec{\alpha}_N)}{\sum_N\sum_{\vec{\alpha}_N}\int \mathrm{d}W(s;\vec{\alpha}_N)} \tag{12}$$

by summing up all channels and integrating over the unobserved variables. Here, the inelastic NN cross section $\sigma_{\text{in}}(s)$ serves as normalization.

For the present considerations the following fixed set of parameter values is used:

$$\begin{array}{rcccl} & & \Theta_I & \equiv & \Theta = 300\,\text{MeV} \\ R_N & = & R_I & \equiv & R = 1.7\,\text{fm} \\ & & & & \beta = 3\,\text{GeV}^{-2} \\ & & \overline{Q}_I & \equiv & \overline{Q} = 400\,\text{MeV/c} \\ & & & & \lambda = 0.15\,. \end{array} \tag{13}$$

2.2. Nucleus-nucleus interactions

In the ROC model a nucleus-nucleus reaction is described on the basis of the participant–spectator picture (at the nucleon level). Each interaction of the projectile nucleus (AZ_A) consisting of A nucleons and Z_A protons with the target nucleus (BZ_B) is characterized by the numbers a (b) and z_A (z_b) of projectile (target) nucleons and of projectile (target) protons involved in the reaction. After the separation of the spectators consisting of $C = A - a$ and $D = B - b$ nucleons it remains the participant interaction, which is treated in close analogy to the nuceon-nuceon interaction described in Sect. 2.1. As an additional aspect light fragments (deuterons, tritons and so on) may emerge from the subsystems if the number of initial valence quarks is sufficient. Nucleons may also coalesce into fragments via final-state interactions. The structure of the residual nucleus is disturbed by the primary projectile-participant reactions as well as by secondary interactions of the outgoing particles with the nuclear environment. That means that the residual nucleus becomes excited too and may break into several fragments. The cross sections σ_{ab} for the interaction of a projectile nucleons with b target nucleons are calculated on the basis of a probabilistic interpretation of the Glauber theory [6] (for details see [14]). Simple combinatorics is then used to calculate the cross sections $\sigma_{az_abz_b}$ which take into account the different charge states z_a, z_b of the participating nucleon groups. The differential cross section is calculated as an incoherent sum

$$\mathrm{d}\sigma_{AB}(s;\vec{\alpha}) = \sum_a \sum_{z_a} \sum_b \sum_{z_b} \sigma_{az_abz_b} \frac{\mathrm{d}W_{az_abz_b}(s;\vec{\alpha}_N)}{\sum_{\vec{\alpha}} \int \mathrm{d}W_{az_abz_b}(s;\vec{\alpha}_N)} \tag{14}$$

with s denoting the square of the CM energy of the projectile-target system. In (14) the relative probability $\mathrm{d}W_{az_abz_b}(s;\vec{\alpha}_N)$ of populating the channel $\vec{\alpha}_N = (\alpha_1, \ldots, \alpha_N, \alpha_C, \alpha_D)$ is given by

$$\mathrm{d}W(s;\vec{\alpha}_N) \propto \mathrm{d}\mathcal{Z}_C(\alpha_C)\mathrm{d}\mathcal{Z}_D(\alpha_D) \left\{ \prod_{i=1}^{N} \mathrm{d}\mathcal{Z}_I(\alpha_I) \right\} \mathrm{d}\mathcal{Z}_N(s'), \tag{15}$$

with $\mathrm{d}\mathcal{Z}_I(\alpha_I)$ and $\mathrm{d}\mathcal{Z}_N(s')$ defined by (9) and (10), while the spectator system J ($J = C, D$) is described by

$$\mathrm{d}\mathcal{Z}_J(\alpha_J) = \mathrm{d}M_J^2 \frac{\mathrm{d}^3P_J}{E_J} \rho_A(\vec{P}_J^2) \left\{ \prod_{i=1}^{n_J} (2\sigma_i + 1) 2m_i \mathrm{d}m_i F_i(m_i) \right\}$$
$$g(\alpha_J) \left(\frac{V_J}{(2\pi)^3} \right)^{n_J - 1} \left(\frac{M_J}{\Theta_J} \right) K_1 \left(\frac{M_J}{\Theta_J} \right) \mathrm{d}L_{n_J}(M_J; \alpha_J) \quad (16)$$

in analogy to (9). New features compared to the NN case are the integral over the internal momentum distribution $\rho_A(\vec{P}_J^2)$ and the function $F_i(m_i)$, which defines the level density of the i-th nuclear fragment.

The parameters β and $\overline{Q}$ [see (6)] are adapted to the peculiarities of a nuclear interaction. It must be expected that the predominantly longitudinal population of the phase-space in hadronic interactions becomes more and more isotropic with increasing number of participants a and b in nuclear reactions. To reproduce this feature the values from the NN case, $\beta = 3\mathrm{GeV}^{-2}$ and $\overline{Q} = 0.4\mathrm{GeV/c}$, are replaced by functions of the number of participants, namely $\beta = 3(a+b-1)^{-3/2}\mathrm{GeV}^{-2}$ and $\overline{Q} = 0.4(a+b-1)^{3/2}\mathrm{GeV/c}$. The calculated spectra are not very sensitive to the details of the selected functional dependence, and the scaling with the number of participants should be considered as one possibility to achieve a reasonable description of the data. For the temperature parameters of the spectator systems values around 5 MeV are used.

3. Comparison with experimental results

In this section a few examples are discussed, which demonstrate the ability of the model to reproduce experimental data in wide regions of incident energy and types of interacting particles.

In a recent paper [1] the total cross sections for various inclusive and exclusive particle production channels in pp interactions at energies up to 50 GeV has been considered. In Fig. 1 the equivalent result for pn reactions is shown. The overall reproduction of the data is quite satisfactory. It is not the aim to discuss all depicted channels thoroughly but rather to stress the variety of reactions reaching from exclusive channels with two up to six final particles to inclusive channels and the variety of particles reaching from pions over strange mesons to baryon and meson resonances, which can be described at the same time.

A systematic set of proton-induced reactions [16] on Be, Al, Cu, and Au targets at 14.6 GeV/c has been measured by the E-802 Collaboration at the BNL-AGS. As pointed out by Abott et al. [16] it is the aim of these

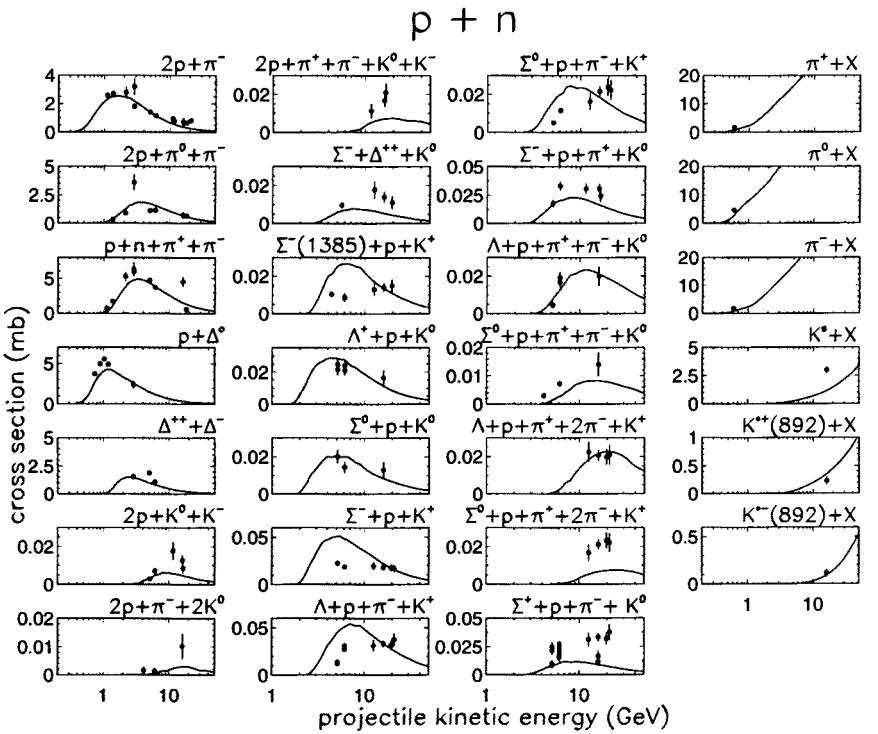

Fig. 1. Energy dependence of the cross section for various particle-production channels in *pn* collisions. Experimental data (*full circles*) from Refs. [15] are compared with ROC model results (*solid lines*).

experiments to clarify the reaction mechanism of nucleus-nucleus (AA) reactions investigated at the same energy per nucleon [17, 18, 19]. In central SiAu interactions an enhanced K^+/π^+ ratio has been observed [18]. This fact is of particular interest, because strangeness production has been discussed in the context of quark-gluon plasma formation [20, 21]. So far, theoretical work [22] – [28] has mainly concentrated on the explanation of the enhanced K^+/π^+ ratio. The comprehensive data set now available is, however, an ideal tool to check models in a more systematic way by considering first pA reactions starting from the lightest systems. After that one can hope to find a more profound explanation of the enhanced K^+/π^+ ratio. In a recent note [2] a first step has been done by calculating the invariant cross sections for the production of $\pi^\pm$, $K^\pm$, p, and d in pBe interactions within the ROC model. Here, the analog results for a heavier target (Al) are presented in Fig. 2, while Fig. 3 shows the rapidity distributions, which follow from the spectra of Fig. 2 by integrating over the transverse kinetic energy $m_t - m_0$. The overall agreement is quite satisfactory.

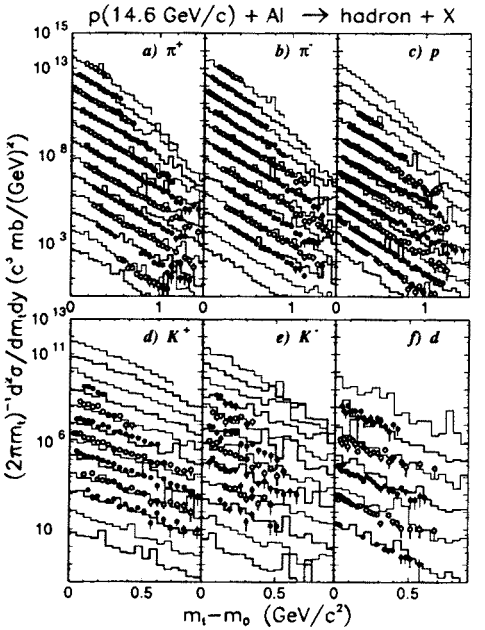

Fig. 2. Invariant cross sections for the production of **a)** π^+, **b)** π^-, **c)** p, **d)** K^+, **e)** K^-, and **f)** d in the rapidity interval $0.4 < y < 2.8$ as a function of $m_t - m_0$ with $m_t = \sqrt{m_0^2 + p_t^2}$ being the transverse mass. Spectra are plotted for a rapidity interval of 0.2 and multiplied by an integral power of 10, that is 10^0 for $0.4 < y < 0.6$, 10^1 for $0.6 < y < 0.8$, etc. For the deuterons in **f)** the spectra are multiplied by powers of 10^2 instead of 10. The experimental data (*open* and *full circles*) [16] are compared with the results of ROC model calculations (*thin* and *thick histograms*).

4. Missing-mass spectra at subthreshold energies

As an example for the application of the ROC model in preparing new experiments the proposed [29] measurement of missing mass spectra is discussed in this section. Subthreshold production of particles is at present far from being understood. Alternative physical pictures are used to interpret the experimental results. The determination of the number of target nucleons participating in the interaction process will be a useful tool to decide between the various approaches. This will be discussed in more detail for the case of subthreshold K^- production, because there are plans [29] to investigate subthreshold K^- production at the spectrometer ANKE [30] at COSY-Jülich.

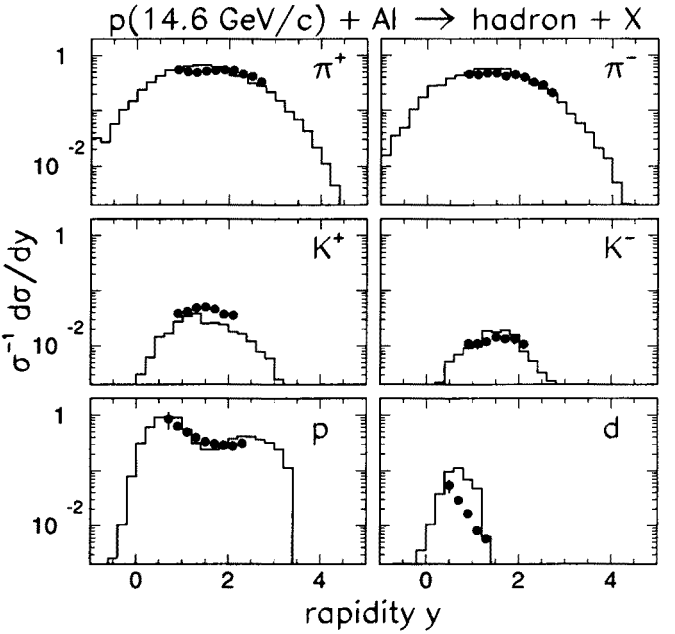

Fig. 3. Rapidity distributions for the production of π^+, π^-, p, K^+, K^-, and d. The experimental data (*full circles*) [16] are compared with the results of ROC model calculations (*histograms*)

In the process

$$p + [aN] \rightarrow (a+1)N + K^+ + K^- \quad (a = 1 \ldots A) \tag{17}$$

with a being the number of participants an energy of about 1 GeV is transferred. Most of this energy is necessary to create the kaon pair. Only a small amount of the available energy remains as relative energy between the $(a+1)$ nucleons and the two kaons in the rest system of this particle group. Thus, the velocity of all particles originating from the participant interaction is in the laboratory system quite close to the (high) velocity of their rest system itself. Because the energy transfer to the remaining $(A-a)$ spectator nucleons is comparably small, their relative velocities as well as the velocity of their rest system in the laboratory remain small. Therefore, a kinematic distinction between these two groups of particles is possible. The recipe for fixing the number of participants is quite obvious, one has to measure all fast particles (kaons, nucleons, fragments), which at subthreshold energies are emitted under small angles in the laboratory system. In the missing-mass spectra peaks must appear, which correspond to the masses of the spectator systems consisting of the residual $(A-a)$ nucleons, if all fast particles are measured. If one or several of the fast particles

are missed then they increase the corresponding missing mass and the peaks are accompanied by tails at the high-mass side. Therefore it is necessary to measure the momenta of all fast particles with an accuracy sufficient for separating the peaks from the accompanying background.

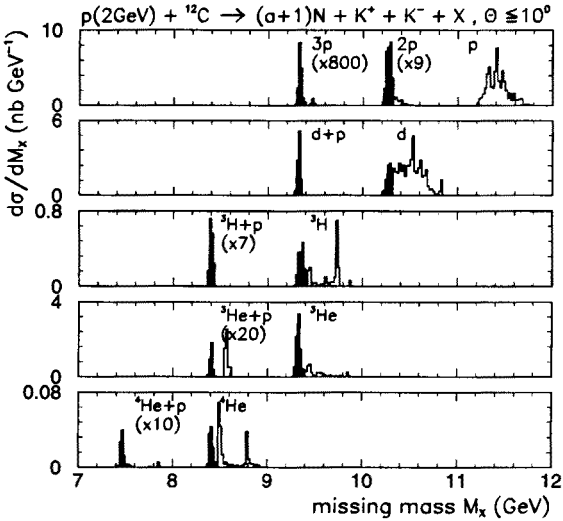

Fig. 4. Calculated missing mass spectra from p^{12}C interactions at 2.0 GeV for the production of K^+/K^- pairs accompanied by $(a+1)$ nucleons with a being the number of participants (see Eq.(17)). Type and number of the nucleonic ejectiles are indicated. Some of the histograms are multiplied by factors given in parentheses

As an illustration missing-mass spectra calculated with the ROC model for p^{12}C interactions at 2.0 GeV are plotted in Fig. 4. It is assumed that all charged particles emitted under angles $\Theta \leq 10°$ are "measured" with 100% efficiency and with a momentum resolution of $\Delta p/p = 1.5\%$. There are peak positions at about 10.2, 9.3, 8.4 and 7.5 GeV, which correspond to spectator systems consisting of eleven to eight nucleons, respectively. The peak denoted by "$2p$" arises from the interaction of the projectile with a single target proton according to

$$p + [p] \rightarrow p + p + K^+ + K^-. \tag{18}$$

The tail at the right side of this peak in Fig. 4 indicates the presence of processes with additional fast particles involved, which are not detected. One such process, denoted by "$3p$", originates from the interaction with a two-nucleon cluster $[2p]$

$$p + [2p] \rightarrow 3p + K^+ + K^-. \tag{19}$$

The peak denoted by "d" comes from the interaction of the projectile with a single target neutron and subsequent coalescence of the p and the n into a d

$$p + [n] \rightarrow p + n + K^+ + K^- \rightarrow d + K^+ + K^-. \tag{20}$$

Here, the distinguished bump arises mainly from additional protons emerging in the process labeled by "$d + p$". The effective target in this case is a $[pn]$ cluster, which can form a d directly

$$p + [pn] \rightarrow p + d + K^+ + K^- \tag{21}$$

or again via coalescence

$$p + [pn] \rightarrow p + p + n + K^+ + K^- \rightarrow p + d + K^+ + K^-. \tag{22}$$

The extension of this discussion to all other processes from Fig. 4 is straightforward.

So far, subthreshold particle production has been investigated by inclusive measurements. In such experiments the various subprocesses cannot be identified in a model-independent way, because inclusive momentum spectra contain no peculiarities which would allow this. In contrast, the positions of the expected peaks in the missing-mass spectra are clearly model independent, while the calculation of the relative intensity of the various subprocesses is a critical measure, which depends on the model approach. Thus, a measurement of missing-mass spectra opens a new way to study details of particle production processes so far unaccessible at medium energies.

5. Conclusions

The ROC model offers the possibility of a simultaneous description of all reaction channels and can be understood as an approach complementary to the usual way of describing a definite reaction channel by means of Feynman diagrams. It is implemented as a generator sampling complete events. This allows the comparison of model calculations with any kind of experimental results as well as the application as event generator for the preparation and simulation of new experiments.

REFERENCES

[1] H. Müller, *Z. Phys.* **A353**, 103 (1995).
[2] H. Müller, *Z. Phys.* **A353**, 237 (1995).
[3] E. L. Feinberg, *Usp. Fiz. Nauk* **104**, 539 (1971).

[4] E. L. Feinberg, *Usp. Fiz. Nauk* **139**, 3 (1983).
[5] G. Giacomelli, *Int. J. Mod. Phys.* **5**, 223 (1990).
[6] R. J. Glauber, J. Mathiae, *Nucl. Phys.* **B21**, 135 (1970).
[7] A. Capella, U. Sukhatme, C.-I. Tan, J. T. T. Van, *Phys. Rep.* **236**, 225 (1994).
[8] E. Byckling, K. Kajantie, *Particle Kinematics*, John Wiley and Sons, London, New York, Sydney, Toronto 1973.
[9] K. Goulianos, *Phys. Rep.* **101**, 169 (1983).
[10] V. Vrba, *Comput. Phys. Commun.* **56**, 165 (1989).
[11] V. V. Anisovich, V. M. Shekhter, *Nucl. Phys.* **B55**, 455 (1973).
[12] L. Montanet *et al.*, *Phys. Rev.* **D50**, 1173 (1994).
[13] H. Müller, *Z. Phys.* **A336**, 103 (1990).
[14] S. Shmakov, V. Uzhinskii, A.M.Zadorozhny, *Comput. Phys. Commun.* **54**, 125 (1988).
[15] V. Flaminio, W. Moorhead, D. Morrison, N. Rivoire, Compilation of cross-sections iii: p and $\bar{p}$ induced reactions. Tech. Rep. CERN-HERA 84-01, CERN (1984).
[16] T. Abbott *et al.*, *Phys. Rev.* **D45**, 3906 (1992).
[17] T. Abbott *et al.*, *Phys. Lett.* **B197**, 285 (1987).
[18] T. Abbott *et al.*, *Phys. Rev. Lett.* **64**, 847 (1990).
[19] J. Barrette etal, *Phys. Rev. Lett.* **64**, 1219 (1990).
[20] J. Rafelski, *Phys. Rep.* **88**, 331 (1982).
[21] P. Koch, B. Müller, J. Rafelski, *Phys. Rep.* **142**, 167 (1986).
[22] J. Cleymans, H. Satz, E. Suhonen, D. von Oertzen, *Phys. Lett.* **B242**, 111 (1990).
[23] C. M. Ko, L. Xia, *Phys. Rev.* **C38**, 179 (1988).
[24] C. M. Ko, L. Xia, *Nucl. Phys.* **A498**, 561c (1989).
[25] R. Mattiello, H. Sorge, H. Stöcker, W. Greiner, *Phys. Rev. Lett.* **63**, 1459 (1989).
[26] C. Wei-qin, G. Chong-shou, Z. Yun-lun, *Nucl. Phys.* **A514**, 734 (1990).
[27] Y. Pang, T. J. Schlagel, S. H. Kahana, *Phys. Rev. Lett.* **68**, 2743 (1992).
[28] Y. Pang, T. J. Schlagel, S. H. Kahana, *Nucl. Phys.* **A544**, 435c (1992).
[29] T. Kirchner *et al.*, COSY Proposal #21 Jülich (1996).
[30] O. W. B. Schult *et al.*, *Nucl. Phys.* **A583**, 629 (1995).